Accurate and Precise Determination of Mechanical Properties of Silicon Nitride Beam Nanoelectromechanical Devices

Accurate and Precise Determination of Mechanical Properties of Silicon Nitride Beam Nano-electromechanical Devices

Hakseong Kim,[†, ▽] *Dong Hoon Shin,*[‡, ▽] *Kirstie McAllister,*[‡, ▽] *Miri Seo,*[‡] *Sangik Lee,*[§] *Il-Suk Kang,*[⊥] *Bae Ho Park,*[§] *Eleanor E. B. Campbell,*[∥, §] *and Sang Wook Lee*[‡,*]

[†]Korea Research Institute of Standards and Science (KRISS), Daejeon 34113, Korea

[‡]Department of Physics, Ewha Womans University, Seoul 03760, Korea

[§]Division of Quantum Phases & Devices, School of Physics, Konkuk University, Seoul 05029, Korea

[⊥]National Nanofab Center, Korea Advanced Institute of Science and Technology, Daejeon 34141, Korea

[∥] EaStCHEM, School of Chemistry, Edinburgh University, David Brewster Road, Edinburgh EH9 3FJ, UK

KEYWORDS

Nano-electromechanical systems, resonators, mass sensors, biomolecular sensors, gas detectors

ABSTRACT

Accurate and precise determination of mechanical properties of nanoscale materials is mandatory since device performances of nano-electromechanical systems (NEMS) are closely related to the flexural properties of the materials. In this study, the intrinsic mechanical properties of highly stressed silicon nitride (SiN) beams of varying lengths are investigated using two different techniques: Dynamic flexural measurement using optical interferometry and quasi-static flexural measurement using atomic force microscopy. The resonance frequencies of the doubly-clamped, highly stressed beams are found to be inversely proportional to their length, which is not usually observed from a beam but is expected from a string-like structure. The mass density of the SiN beams can be precisely determined from the dynamic flexural measurements by using the values for internal stress and Young's modulus determined from the quasi-static measurements. As a result, the mass resolution of the SiN beam resonators was predicted to be a few atto-grams, which was found to be in excellent agreement with the experimental results. This work suggests that accurate and precise determination of mechanical properties can be achieved through combined flexural measurement techniques, which is a crucial key for designing practical NEMS applications such as biomolecular sensors and gas detectors.

INTRODUCTION

In recent years, nano-electromechanical resonators have been the focus of numerous studies due to their desirable properties such as low energy consumption,[1,2] rapid response time,[3] high sensitivities[4] and ease of integration.[5] As a result of the interest shown by both experimental and theoretical researchers,[6-8] advances in both fundamental and applied science have been achieved through realization of nano-electromechanical systems (NEMS) such as non-volatile memory devices with high speed operation,[9] frequency tunable RF receivers,[10-12] power generators for energy harvesting[13] and ultra-sensitive mass detectors.[14-19] Moreover, computational simulations support technical advances in NEMS by predicting and understanding the atomic or molecular interactions and flexural behaviors in NEMS.

Among many materials deemed suitable for NEMS applications, highly stressed silicon nitride (SiN) has been considered one of the most promising candidates for realizing NEMS based high performance sensing devices. The mechanical properties of SiN, in particular high frequency operation and high quality factors,[20,21] lend themselves well for using this material as sensitive mass,[22,23] temperature[24] or quantum motion detectors.[25] Due to the increased elastic energy, pre-stressed SiN based NEMS have high quality factors,[26] hence sensitive device operation can be achievable even at room temperature.[20] Doubly-clamped SiN beams have string-like properties with a simple bending mode shape function that makes them particularly suitable as mass sensors.[21,22,27]

However, NEMS based high performance sensors are made possible only through intensive study and understanding of the intrinsic mechanical properties of materials, since device performances of NEMS are closely related to the flexural properties of the materials from which they are fabricated. The mass sensitivity of SiN resonators should be inversely proportional to

their mass, and it is therefore important to determine the mechanical properties accurately and precisely as the beam dimensions are reduced in order to establish a practical mass detection limit. Thus, accurate and precise characterization of basic mechanical properties such as Young's modulus[28,29] and intrinsic tensile stress[30] of materials at the nanoscale are crucial factors for designing NEMS structures whose motions can be accurately and reliably predicted.

In this paper, the length dependence of the mechanical properties of highly stressed SiN beams was investigated by both dynamic[31,32] and quasi-static[32,33] flexural measurement techniques, which are well suited for non-destructive inspection and study of the fundamental elastic properties of materials. The mass density, Young's modulus and internal stress of the SiN beams were extracted from a combination of the two different flexural measurement techniques. In order to evaluate the accuracy and reliability of these determined values, the mass responsivities of the SiN beams were estimated using determined values and then compared with the experimental values which were obtained by observing the change in resonance frequency after controlled deposition of chromium (Cr).

EXPERIMENTAL SECTION

Device fabrication. The details of device fabrication are as follows; (i) a 200 nm thick plasma enhanced chemical vapor deposition (PECVD) grown high stress SiN film was prepared on a SiO_2/Si wafer.[34] (ii) Polymethylmethacrylate (PMMA) C4 was spin-coated on the substrate at 4500 rpm followed by baking at 180 °C for 5 minutes. An electron beam dose of 250 μC/cm^2 was used to define a doubly clamped beam shaped pattern on the PMMA layer using electron beam lithography. Then 30 nm of Cr was evaporated on to the substrate as a protective mask for the SiN beams. (iii) After lift-off, reactive ion etching was performed to etch away 200 nm of the

unprotected SiN layer. A 9:1 mixture of CF_4 and O_2 gases (100 W, 20 mTorr) was used for 15 minutes. The Cr layer on top of the SiN beam was removed by putting this substrate in Cr-7 etchant solution. (iv) 500 nm thick SiO_2 sacrificial layer was etched in buffered oxide etchant solution (6:1) for 7 minutes. (v) Finally, a critical point dryer was used to prevent structural collapse of the suspended SiN beams during the drying process.[35]

Dynamic flexural measurement. The dynamic flexural measurements were carried out at room temperature and in a low vacuum condition of around 3×10^{-3} Torr. The SiN beams were actuated by mechanical stimuli induced from the vibration of a piezo-ceramic located underneath the substrate.[13] When the AC frequency applied to the piezo-ceramic matches the mechanical resonance frequency of the SiN beam, the beam exhibits resonance behavior. An optical interferometry technique, suitable for detecting resonance behavior of insulating devices, was employed to detect the vibrational motion.[36,37] The intensity of the He-Ne laser used for the interferometry measurements was set to around 80 μW to minimize heating effects or structural deformation of the beams.[27,38]

Quasi-static flexural measurement. The quasi-static flexural measurements were performed using atomic force microscopy (AFM, Park NX10, Park Systems) based force-distance spectroscopy. The relationship between the force applied by the probe tip and the deflection of the SiN beam was shown to follow Hooke's law.

RESULTS AND DISCUSSION

Figure 1a illustrates the fabrication procedure used to produce the SiN resonators by a standard top-down lithography technique as described in the Experimental Section. Figure 1b shows a scanning electron microscope (SEM) image of a xylophone-like array structure which is

composed of SiN beams with lengths varying from 2 μm to 24 μm, with a fixed width of 750 nm, a thickness of 200 nm and a taper angle of about 10^{o}. All of the SiN beams were well suspended without any deformation or slack. The inset of Figure 1b shows an optical microscope image of the fabricated SiN beam array.

The elastic mechanical properties of the free-standing SiN beams were firstly investigated by dynamic flexural measurement through detection of the resonance frequency of the beams. Figure 2a shows the representative resonance behavior of a 24 μm long SiN beam. The resonance frequency of the fundamental mode was detected to be 12.122 MHz by taking the peak position of the maximum amplitude from a Lorentzian fit curve, shown in Figure 2a as a solid red line. The quality factor is estimated to be around 31000. This value is much higher than those observed in conventional silicon devices.[31,35,37] The presence of high stress within these beams, imparted during SiN film growth using PECVD, leads to both high resonance frequencies and high Q factors, both of which are desirable parameters for a high performance NEMS device.

Figure 2b shows the Q factor dependence on the beam length. It is clearly seen that the Q factors decline from around 30000 to 2400 as the beam length decreases. This phenomenon can be explained by an increase of undercut effect during vibration which is formed by isotropic wet etching process in buffered oxide etchant solution.[21] Since maximum tensile stress and destructive thermal stress of the vibrating beam are mainly generated at the both ends of the beam near the clamping areas, a damping of vibration resulting from partial absence of rigid posts under the clamping regions leads to energy dissipation as the beam length decreases.[38]

The resonance frequencies of SiN beams with lengths from 4 μm to 24 μm are presented in Figure 2c. The shorter beams show higher resonance frequencies as expected. According to

standard beam theory, the formula for a doubly clamped beam under tensile stress can be described by

$$f_0 = 1.03\left(\frac{t}{L^2}\right)\sqrt{\frac{E}{\rho}}\sqrt{1+\frac{\sigma_{int}L^2}{3.4Et^2}} \quad (1)$$

where f_0, t, L, ρ, σ_{int} and E represent the first order resonance frequency, thickness, length, mass density, internal stress and Young's modulus, respectively.[20,32,39] This formula is suitable for estimating the elastic properties of a doubly clamped beam under stress by considering the effects of both the Young's modulus and the tensile stress.

In the case of low stress doubly clamped SiN beams, the frequency variation upon length is seen to follow the tendency of ordinary unstressed beams where the frequency is inversely proportional to the length squared, since the Young's modulus is the dominant factor for determining a beam's elasticity rather than the applied stress.[37] On the other hand, as clearly seen in Figure 2c, highly stressed beams such as the SiN beams studied in this report exhibit string-like resonance behavior where the resonance frequency is inversely proportional to the length since the tensile stress becomes the dominant factor,[21] which is in good agreement with the resonance frequencies reported by Unterreithmeier et al.[27] This confirms that elastic properties of SiN beams with quasi-1-dimensional string-like behavior are more affected by the applied tensile stress than by the Young's modulus.[21,32] For this reason, eq 1 can be simplified to eq 2 by ignoring the Young's modulus term.

$$f_0 = 1.03\sqrt{\frac{1}{3.4\rho}\sigma_{int}}\,L^{-1} \quad (2)$$

Since the beams exhibit such behavior, their resonance frequencies can be reliably predicted with a knowledge of only the length and tensile stress, or the tensile stress in the SiN beams can be estimated from the dependence of the resonance frequency on the beam length.

Generally, the mass density of PECVD grown SiN film is known to be around 2400-2800 kg/m^3, within the stress range of -600 (compressive) to 600 MPa (tensile).[40] A high tensile stress film is expected to have a relatively lower mass density than a low stress film. By considering the value of 270±6 Hz·m which is the linear fit of the slope in Figure 2c, the tensile stress can be estimated to be in the range of 561±22 MPa to 654±26 MPa using eq 2 by assuming a mass density in the range of 2400-2800 kg/m^3. As shown in Figure 2c inset, the extracted value of the tensile stress increases as the assumed mass density value increases, because stress and mass density have a proportional relationship, according to eq 2.

The mechanical elastic properties of the beams were also investigated by a quasi-static method using atomic force microscopy (AFM) force-distance measurements. Figure 3a shows the representative deflection curve of a 22 μm long SiN beam. The relationship between the force applied by the probe tip and the deflection of the SiN beam is shown to follow Hooke's law. From the straight line fit in Fig. 3a, the spring constant of the beam was determined to be 14.09±0.03 N/m. (Inset of Figure 3a shows an AFM topography image of the SiN beam.)

As shown in Figure 3b, the spring constants of the beams increase from 12.5 to 74.2 N/m as the suspended lengths decrease from 24 to 8 μm. For small bending displacements, the analytical model for deflection of a stressed doubly clamped beam loaded at the mid-point can be described with a linear relationship between force and displacement, given by

$$F = \left(\frac{4T}{L} + \frac{192EI}{L^3}\right)\delta, \quad I = \frac{wt^3}{12} \tag{3}$$

where F, δ, T, w and I represent the applied force from the AFM probe tip, deflection of beam, tension, beam width and moment of inertia, respectively.[41,42]

The spring constant consists of a combination of two elements related to stress ($k_{\sigma int}$) and Young's modulus (k_E) as a function of L^{-1} and L^{-3}, respectively. $k_{\sigma int}$ is related to the elastic properties for a stretched string, and k_E is related to the bending moment of a rigid body. In the case of a SiN beam, both components should be considered to be precise estimations of its elastic properties due to its mechanical bending behavior. By considering the Poisson's ratio (v) and the moment of inertia for a rectangular cross-section in eq 3, the formula can be re-written as eq 4.

$$k = \frac{F}{\delta} = k_{\sigma int} + k_E = \frac{4\sigma(1-v)tw}{L} + \frac{16Ewt^3}{L^3} = \frac{A}{L} + \frac{B}{L^3} \tag{4}$$

The experimental data in Figure 3b is fitted to a cubic polynomial curve function with A = 2.67 × 10^{-4} N and B = 1.83 × 10^{-14} N·m^2 in eq 4, respectively. Figure 3c shows the resulting contributions of both the stress ($k_{\sigma int}$) and the Young's modulus (k_E) to the spring constant of the SiN beams. By considering the Poisson's ratio of 0.24 for SiN,[43] we were able to determine the stress and Young's modulus of the SiN beams to be 585±8 MPa and 190±16 GPa, respectively. It can be shown that as the beam lengths are decreased, the Young's modulus becomes a more dominant factor for defining the elastic spring constant than the stress. Our extracted value of the Young's modulus is consistent with the range of previously reported values.[34,43,44] Also, the tensile stress range determined by the quasi-static flexural measurements is consistent with the above results from the dynamic flexural measurement but with lower uncertainty limits. It is

therefore possible to use these limits in the dynamic flexural analysis to more accurately determine the mass density of the beams to be within the range 2365-2635 kg/m^3.

From the results of both measurements, the mass density, tensile stress and Young's modulus of the SiN beams were accurately determined to be 2500±135 kg/m^3, 585±8 MPa and 190±16 GPa, respectively. Thanks to the complementary measurement techniques, the determined values could be cross-checked. Since both of the measurement techniques are based on non-destructive inspection, those accurate values can be used directly for estimation of the device performance.

In order to investigate the accuracy and reliability of the determined values, mass responsivities of our SiN devices were obtained through observing resonance frequency shifts induced by mass loading after evaporation of Cr on to 14 μm and 22 μm long beams at the same time, using electron beam evaporation. The masses loaded were estimated to be around 0.82 fg and 1.3 fg for 14 μm and 22 μm long SiN beams, respectively, by considering the SiN surface area, the taper angle, the deposition thickness and the mass density of the Cr.[45] As shown in Figure 4a, the resonance frequencies of both beams downshifted after each successive evaporation, which fits to a line with only a small amount of deviation. This result indicates that approximately the same mass of Cr was evaporated on beam surfaces for each metal evaporation step. Based on this experimental result, mass responsivities of 14 μm and 22 μm devices were determined to be 0.35±0.01 ag/Hz and 0.86±0.05 ag/Hz, respectively, where the shorter beam has a better mass responsivity than the longer beam.

The mass responsivities of 4 μm to 24 μm beams were estimated using a simple analytical model shown in eq 5

$$\delta m = -\frac{2M_{eff}}{f_0}\delta f = R_m \delta f \tag{5}$$

where δm, M_{eff}, f_0, δf and R_m represent the minimum detectable mass, effective mass of the beam, resonance frequency, frequency deviation and mass responsivity, respectively.[46] For a doubly clamped beam, the M_{eff} is $0.735lwt\rho$.[47]

Figure 4b shows the variation of mass responsivity calculated using eq 5 as the length is down-scaled with the mass density set to be 2500±135 kg/m^3, as determined by the flexural measurements. Furthermore, from the dynamic flexural measurements, the resonance frequencies of the 14 μm and 22 μm beams were determined to be 21.4 MHz and 14.0 MHz, respectively. The inset of Figure 4b represents the effective mass and the resonance frequency as a function of inverse length.

If we assume that the resonance frequencies of the devices show the exactly same values for several successive measurements, and that a frequency shift can only be observed by additional mass loading, the minimum detectable masses for lengths of beam from 24 to 4 μm are in the range of 1.04 ag to 0.033 ag due to a decrease in M_{eff} and an increase in f_0 where the frequency deviation δf is set to 1 Hz. From this estimation, mass responsivities for 14 μm and 22 μm beams were determined to be 0.36±0.02 ag/Hz and 0.87±0.05 ag/Hz, respectively. These results are very close to the experimentally-determined mass responsivities of 0.35±0.01 ag/Hz for the 14 μm beam and 0.86±0.05 ag/Hz for the 22 μm beam.

According to eq 5, it is necessary to reduce the values of M_{eff} and δf while increasing the value of f_0 in order to enhance the sensitivity of a NEMS based mass sensor. To satisfy these conditions, down-scaling of the devices is required which can accomplish both high resonance frequency and low effective mass. However, in a practical situation, some frequency fluctuations of the same beam, caused by energy dissipation during vibration, are observed by performing

consecutive resonance frequency measurements. Therefore, to define the minimum detectable mass, a frequency shift induced by the loading of mass should be larger than the range of frequency fluctuation produced by energy dissipation.[14,46] In light of this, we determine δf in eq 5 as the standard deviation of averaged resonance frequencies from five repeated measurements for each beam. The 22 μm long SiN beam shows a relatively low frequency deviation of 2.74 Hz, but the 14 μm beam has a much greater frequency deviation of 34.84 Hz, as shown in Figure 4c, due to the fairly low Q factors discussed earlier. When δf was considered as a parameter to determine the mass sensitivities for each beam, the 22 μm long beam exhibits a minimum detectable mass of 2.4±0.1 ag which is 5 times more sensitive than the 12.3±0.5 ag minimum detectable mass of the 14 μm beam. By considering that these experiments were carried out at low vacuum and room temperature, a mass resolution of a few atto-grams is a remarkable performance for a mass sensor. It is also noteworthy that the performance of the NEMS device was predicted accurately and reliably by virtue of the accurate and precise determination of the mechanical properties.

CONCLUSIONS

In this study, the mechanical properties of PECVD grown SiN beams were determined by two non-destructive inspection techniques, namely dynamic flexural measurements and quasi-static flexural measurements. The Young's moduli and internal stress values of the SiN beams were accurately determined from the quasi-static measurement. The mass density of the SiN was estimated from the experimentally-determined stress values obtained from the dynamic measurements. From the results of these studies, mass density, tensile stress and Young's moduli of the SiN beams could be accurately and precisely determined to be 2500±135 kg/m^3, 585±8

MPa and 190±16 GPa, respectively. By using these experimentally-determined values, the mass resolution of practical, down-scaled NEMS devices was estimated to be around a few atto-grams. This type of study can be widely used for determining the exact ranges of material properties required to design NEMS devices such as biomolecular sensors and gas detectors with highly predictable and reliable behavior.

ACKNOWLEDGMENT

This research was supported by the Basic Science Research Program (NRF-2015R1A2A2A05050829), the Quantum Metamaterials Research Center Program (No. 2015001948) and the Nano·Material Technology Development Program (2012M3A7B4049888) through the National Research Foundation of Korea (NRF) funded by the Korea government (MSIP). This research was also financially supported by the Ministry of Trade, Industry and Energy (MOTIE) and Korea Institute for Advancement of Technology (KIAT) through the International Cooperative R&D program.

AUTHOR INFORMATION

Corresponding Author

*E-mail: leesw@ewha.ac.kr (S. W. Lee).

Author Contributions

▽H. K., D. H. S. and K. M. contributed equally to this work. H.K, D.H.S, E.E.B.C and S.W.L conceived the idea and analyzed the data. H.K and K.M carried out the dynamic and quasi-static flexural measurements. H.K, M.S and I.-S.K fabricated the device samples. S.L and B.H.P

contributed to mass loading tests. The manuscript was written with contributions of all authors. All authors have given approval to the final version of the manuscript.

Notes

The authors declare no competing financial interest.

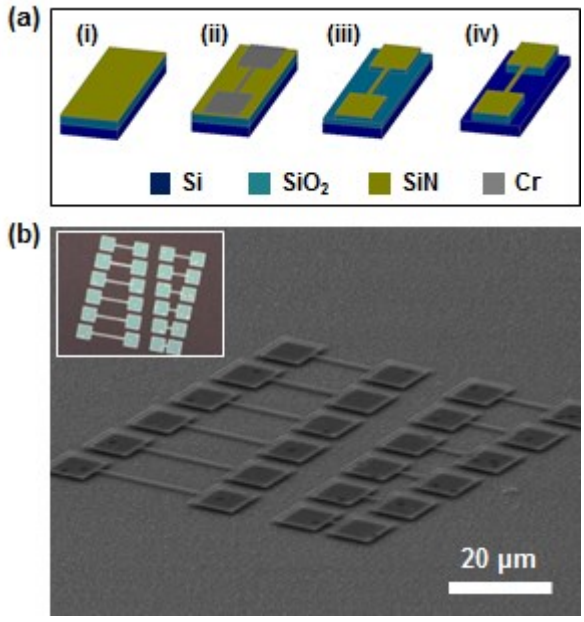

Figure 1. (a) Fabrication procedure for free standing SiN beam. (b) Scanning electron microscope image of SiN device with 2 ~ 24 μm length. Inset shows optical microscope image of SiN beams.

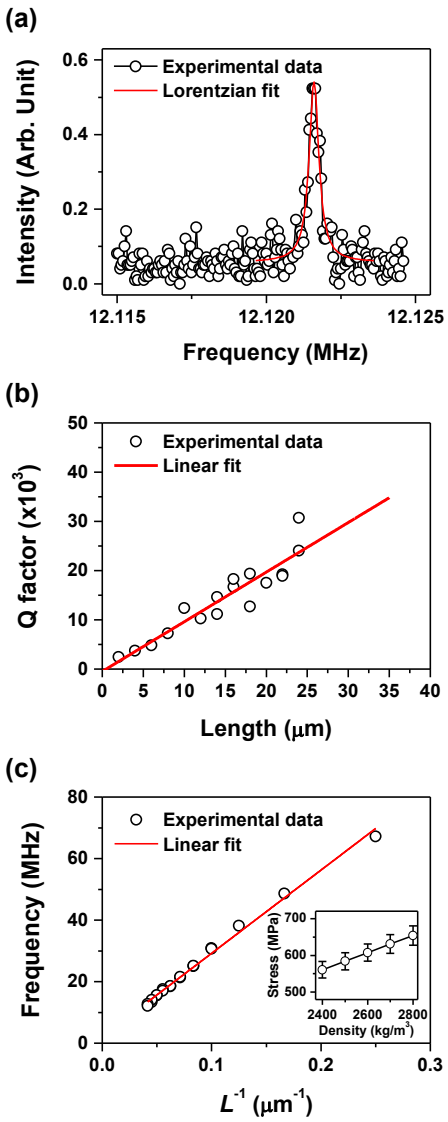

Figure 2. Resonant behavior of SiN beam acquired from dynamic flexural measurement technique. (a) Resonance frequency of 24 μm long SiN beam and its quality factor. (b) Quality factor variation as a function of beam length. (c) Resonance frequency as a function of inverse beam length. Inset shows estimated stress depending on mass density of SiN beam.

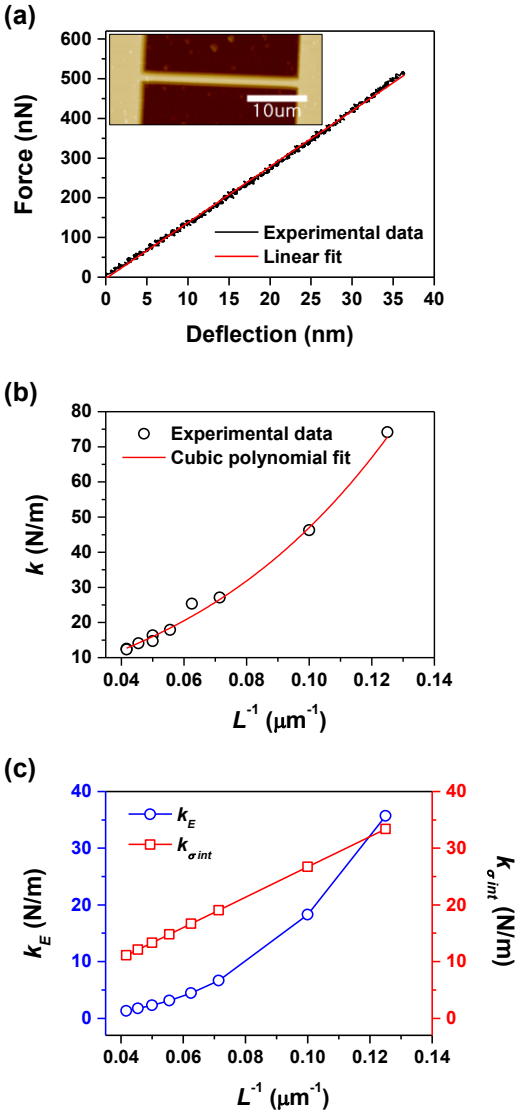

Figure 3. Force-deflection relationship of SiN beam acquired by quasi-static measurement technique (a) representative force-deflection curve of 22 μm long SiN beam. Inset shows AFM image of 22 μm long device. (b) Spring constant as a function of inverse length. (c) Contributions of both the stress (red) and the Young's modulus (blue) to the spring constant of the SiN beams as a function of inverse length.

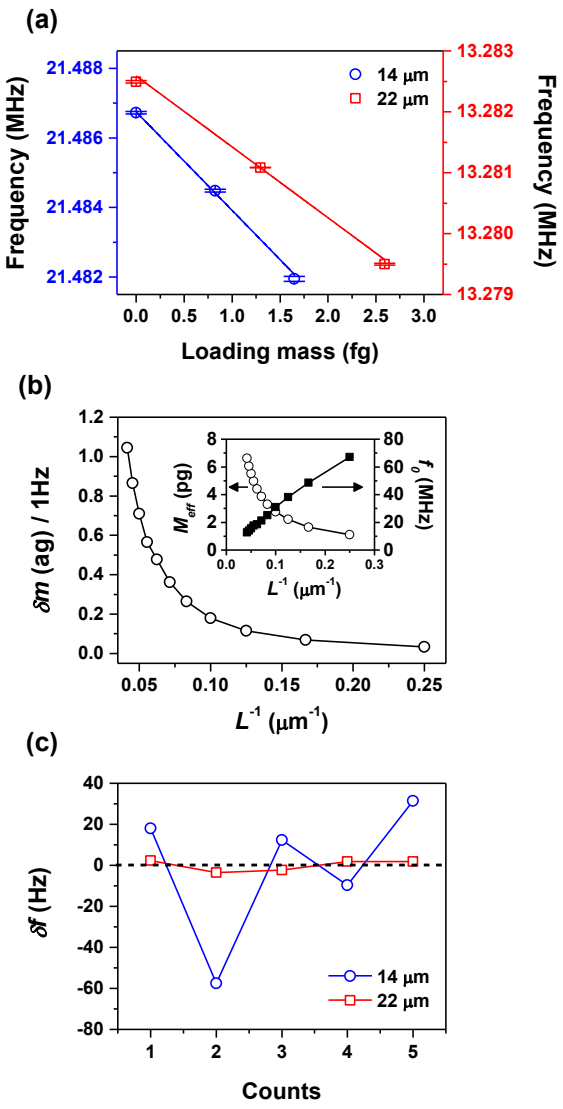

Figure 4. (a) Variation of resonance frequency after loading mass for 14 μm and 22 μm long SiN beams. (b) Estimated mass responsivity as a function of inverse length. Inset shows the effective mass and resonance frequency as a function of inverse length. (c) Comparison of frequency deviation for 14 μm and 22 μm long SiN beams.

REFERENCES

(1) Feng, X. L.; Matheny, M. H.; Zorman, C. A.; Mehregany, M.; Roukes, M. L. Low Voltage Nanoelectromechanical Switches Based on Silicon Carbide Nanowires. *Nano Lett.* **2010,** *10*, 2891-2896.

(2) Bartsch, S. T.; Lovera, A.; Grogg, D.; Ionescu, A. M. Nanomechanical Silicon Resonators with Intrinsic Tunable Gain and Sub-nW Power Consumption. *ACS Nano* **2012,** *6*, 256-264.

(3) Kim, S. M.; Song, E. B.; Lee, S.; Seo, S.; Seo, D. H.; Hwang, Y.; Candler, R.; Wang, K. L. Suspended Few-layer Graphene Beam Electromechanical Switch with Abrupt On-Off Characteristics and Minimal Leakage Current. *Appl. Phys. Lett.* **2011,** *99*, 023103.

(4) Li, M.; Tang, H. X.; Roukes, M. L. Ultra-sensitive NEMS-Based Cantilevers for Sensing, Scanned Probe and Very High-Frequency Applications. *Nat. Nanotechnol.* **2007,** *2*, 114-120.

(5) Bargatin, I.; Myers, E. B.; Aldridge, J. S.; Marcoux, C.; Brianceau, P.; Duraffourg, L.; Colinet, E.; Hentz, S.; Andreucci, P.; Roukes, M. L. Large-Scale Integration of Nanoelectromechanical Systems for Gas Sensing Applications. *Nano Lett.* **2012,** *12*, 1269-1274.

(6) Atalaya, J.; Isacsson, A.; Kinaret, J. M. Continuum Elastic Modeling of Graphene Resonators. *Nano Lett.* **2008,** *8*, 4196-4200.

(7) Jiang, J.-W.; Park, H. S.; Rabczuk, T. Enhancing the Mass Sensitivity of Graphene Nanoresonators via Nonlinear Oscillations: The Effective Strain Mechanism. *Nanotechnology* **2012,** *23*, 475501.

(8) Jiang, J.-W.; Yang, N.; Wang, B.-S.; Rabczuk, T. Modulation of Thermal Conductivity in Kinked Silicon Nanowires: Phonon Interchanging and Pinching Effects. *Nano Lett.* **2013,** *13*, 1670-1674.

(9) Lee, S. W.; Park, S. J.; Campbell, E. E. B.; Park, Y. W. A Fast and Low-Power Microelectromechanical System-Based Non-Volatile Memory Device. *Nat. Commun.* **2011,** *2*, 220.

(10) Eriksson, A.; Lee, S.; Sourab, A. A.; Isacsson, A.; Kaunisto, R.; Kinaret, J. M.; Campbell, E. E. B. Direct Transmission Detection of Tunable Mechanical Resonance in an Individual Carbon Nanofiber Relay. *Nano Lett.* **2008,** *8*, 1224-1228.

(11) Chen, C.; Lee, S.; Deshpande, V. V.; Lee, G.-H.; Lekas, M.; Shepard, K.; Hone, J. Graphene Mechanical Oscillators with Tunable Frequency. *Nat. Nanotechnol.* **2013,** *8*, 923-927.

(12) Sazonova, V.; Yaish, Y.; Üstünel, H.; Roundy, D.; Arias, T. A.; McEuen, P. L. A Tunable Carbon Nanotube Electromechanical Oscillator. *Nature* **2004,** *431*, 284-287.

(13) Kim, H.; Yun, H.; Yoon, H. A.; Lee, S. W. Integrating ZnO Microwires with Nanoscale Electrodes Using a Suspended PMMA Ribbon for Studying Reliable Electrical and Electromechanical Properties. *Adv. Energy Mater.* **2014,** *4*, 1301973.

(14) Chaste, J.; Eichler, A.; Moser, J.; Ceballos, G.; Rurali, R.; Bachtold, A. A Nanomechanical Mass Sensor with Yoctogram Resolution. *Nat. Nanotechnol.* **2012,** *7*, 301-304.

(15) Chen, C.; Rosenblatt, S.; Bolotin, K. I.; Kalb, W.; Kim, P.; Kymissis, I.; Stormer, H. L.; Heinz, T. F.; Hone, J. Performance of Monolayer Graphene Nanomechanical Resonators with Electrical Readout. *Nat. Nanotechnol.* **2009,** *4*, 861-867.

(16) Tao, Y.; Boss, J. M.; Moores, B. A.; Degen, C. L. Single-Crystal Diamond Nanomechanical Resonators with Quality Factors Exceeding One Million. *Nat. Commun.* **2014,** *5*, 3638.

(17) Olcum, S.; Cermak, N.; Wasserman, S. C.; Manalis, S. R. High-Speed Multiple-Mode Mass-Sensing Resolves Dynamic Nanoscale Mass Distributions. *Nat. Commun.* **2015,** *6*, 7070.

(18) Sage, E.; Brenac, A.; Alava, T.; Morel, R.; Dupré, C.; Hanay, M. S.; Roukes, M. L.; Duraffourg, L.; Masselon, C.; Hentz, S. Neutral Particle Mass Spectrometry with Nanomechanical Systems. *Nat. Commun.* **2015,** *6*, 6482.

(19) Hanay, M. S.; Kelber, S.; Naik, A. K.; Chi, D.; Hentz, S.; Bullard, E. C.; Colinet, E.; Duraffourg, L.; Roukes, M. L. Single-Protein Nanomechanical Mass Spectrometry in Real Time. *Nat. Nanotechnol.* **2012,** *7*, 602-608.

(20) Verbridge, S. S.; Shapiro, D. F.; Craighead, H. G.; Parpia, J. M. Macroscopic Tuning of Nanomechanics: Substrate Bending for Reversible Control of Frequency and Quality Factor of Nanostring Resonators. *Nano Lett.* **2007,** *7*, 1728-1735.

(21) Verbridge, S. S.; Parpia, J. M.; Reichenbach, R. B.; Bellan, L. M.; Craighead, H. G. High Quality Factor Resonance at Room Temperature with Nanostrings under High Tensile Stress. *J. Appl. Phys.* **2006,** *99*, 124304.

(22) Schmid, S.; Dohn, S.; Boisen, A. Real-Time Particle Mass Spectrometry Based on Resonant Micro Strings. *Sensors* **2010,** *10*, 8092-8100.

(23) Schmid, S.; Kurek, M.; Adolphsen, J. Q.; Boisen, A. Real-Time Single Airborne Nanoparticle Detection with Nanomechanical Resonant Filter-Fiber. *Sci. Rep.* **2013,** *3*, 1288.

(24) Larsen, T.; Schmid, S.; Grönberg, L.; Niskanen, A. O.; Hassel, J.; Dohn, S.; Boisen, A. Ultrasensitive String-Based Temperature Sensors. *Appl. Phys. Lett.* **2011,** *98*, 121901.

(25) Rocheleau, T.; Ndukum, T.; Macklin, C.; Hertzberg, J. B.; Clerk, A. A.; Schwab, K. C. Preparation and Detection of a Mechanical Resonator near the Ground State of Motion. *Nature* **2010,** *463*, 72-75.

(26) Unterreithmeier, Q. P.; Faust, T.; Kotthaus, J. P. Damping of Nanomechanical Resonators. *Phys. Rev. Lett.* **2010,** *105*, 027205.

(27) Suhel, A.; Hauer, B. D.; Biswas, T. S.; Beach, K. S. D.; Davis, J. P. Dissipation Mechanisms in Thermomechanically Driven Silicon Nitride Nanostrings. *Appl. Phys. Lett.* **2012,** *100*, 173111.

(28) Li, P.; Hu, L.; McGaughey, A. J. H.; Shen, S. Crystalline Polyethylene Nanofibers with the Theoretical Limit of Young's Modulus. *Adv. Mater.* **2014,** *26*, 1065-1070.

(29) Kim, H.; Jung, U. S.; Kim, S. I.; Yoon, D.; Cheong, H.; Lee, C. W.; Lee, S. W. Young's Modulus of ZnO Microwires Determined by Various Mechanical Measurement Methods. *Curr. Appl. Phys.* **2014,** *14*, 166-170.

(30) Lee, C.; Wei, X.; Kysar, J. W.; Hone, J. Measurement of the Elastic Properties and Intrinsic Strength of Monolayer Graphene. *Science* **2008,** *321*, 385-388.

(31) Carr, D. W.; Evoy, S.; Sekaric, L.; Craighead, H. G.; Parpia, J. M. Measurement of Mechanical Resonance and Losses in Nanometer Scale Silicon Wires. *Appl. Phys. Lett.* **1999,** *75*, 920-922.

(32) Bak, J. H.; Kim, Y. D.; Hong, S. S.; Lee, B. Y.; Lee, S. R.; Jang, J. H.; Kim, M.; Char, K.; Hong, S.; Park, Y. D. High-Frequency Micromechanical Resonators from Aluminium–Carbon Nanotube Nanolaminates. *Nat. Mater.* **2008,** *7*, 459-463.

(33) Annamalai, M.; Mathew, S.; Jamali, M.; Zhan, D.; Palaniapan, M. Elastic and Nonlinear Response of Nanomechanical Graphene Devices. *J. Micromech. Microeng.* **2012,** *22*, 105024.

(34) Huang, H.; Winchester, K. J.; Suvorova, A.; Lawn, B. R.; Liu, Y.; Hu, X. Z.; Dell, J. M.; Faraone, L. Effect of Deposition Conditions on Mechanical Properties of Low-Temperature PECVD Silicon Nitride Films. *Mater. Sci. Eng., A* **2006,** *435-436*, 453-459.

(35) Hu, H.; Cho, H.; Somnath, S.; Vakakis, A. F.; King, W. P. Silicon Nano-Mechanical Resonators Fabricated by Using Tip-Based Nanofabrication. *Nanotechnology* **2014,** *25*, 275301.

(36) Ekinci, K. L.; Roukes, M. L. Nanoelectromechanical Systems. *Rev. Sci. Instrum.* **2005,** *76*, 061101.

(37) Baek, I.-B.; Lee, B. K.; Kim, Y.; Ahn, C.-G.; Kim, Y. J.; Yoon, Y. S.; Jang, W. I.; Kim, H.; Lee, S. W.; Lee, S.; Yu, H. Y. The Control of Oscillation Mode in Silicon Microbeams Using Silicon Nitride Anchor. *Appl. Phys. Lett.* **2014,** *105*, 103101.

(38) Trushkevych, O.; Shah, V. A.; Myronov, M.; Halpin, J. E.; Rhead, S. D.; Prest, M. J.; Leadley, D. R.; Edwards, R. S. Laser-Vibrometric Ultrasonic Characterization of Resonant Modes and Quality Factors of Ge Membranes. *Sci. Technol. Adv. Mater.* **2014,** *15*, 025004.

(39) Bunch, J. S.; van der Zande, A. M.; Verbridge, S. S.; Frank, I. W.; Tanenbaum, D. M.; Parpia, J. M.; Craighead, H. G.; McEuen, P. L. Electromechanical Resonators from Graphene Sheets. *Science* **2007,** *315*, 490-493.

(40) Beeby, S.; Ensell, G.; Kraft, M.; White, N. *MEMS Mechanical Sensors*; Artech House: Norwood MA, 2004.

(41) Mulloni, V.; Colpo, S.; Faes, A.; Margesin, B. A Simple Analytical Method for Residual Stress Measurement on Suspended MEM Structures Using Surface Profilometry. *J. Micromech. Microeng.* **2013,** *23*, 025025.

(42) Pruessner, M. W.; King, T. T.; Kelly, D. P.; Grover, R.; Calhoun, L. C.; Ghodssi, R. Mechanical Property Measurement of InP-Based MEMS for Optical Communications. *Sens. Actuators, A* **2003,** *105*, 190-200.

(43) Edwards, R. L.; Coles, G.; Sharpe Jr, W. N. Comparison of Tensile and Bulge Tests for Thin-Film Silicon Nitride. *Exp. Mech.* **2004,** *44*, 49-54.

(44) Zhou, W.; Yang, J.; Li, Y.; Ji, A.; Yang, F.; Yu, Y. Bulge Testing and Fracture Properties of Plasma-Enhanced Chemical Vapor Deposited Silicon Nitride Thin Films. *Thin Solid Films* **2009,** *517*, 1989-1994.

(45) Ohring, M. *The Materials Science of Thin Films*; Academic Press: San Diego CA, 1992.

(46) Lassagne, B.; Garcia-Sanchez, D.; Aguasca, A.; Bachtold, A. Ultrasensitive Mass Sensing with a Nanotube Electromechanical Resonator. *Nano Lett.* **2008,** *8*, 3735-3738.

(47) Ekinci, K. L.; Huang, X. M. H.; Roukes, M. L. Ultrasensitive Nanoelectromechanical Mass Detection. *Appl. Phys. Lett.* **2004,** *84*, 4469-4471.

TABLE OF CONTENTS